

1 Safety factor for structural elements 2 subjected to impulsive blast loads

3 Pierluigi Olmati^{1a*}, Dimitrios Vamvatsikos^{2b}, Mark G. Stewart^{3c}

4 ¹ Department of Architecture and Wind Engineering, Tokyo Polytechnic University, Japan.

5 ² School of Civil Engineering, National Technical University of Athens, Greece.

6 ³ Centre for Infrastructure Performance and Reliability, The University of Newcastle,
7 Australia.

8 ^a Researcher, fellow of the Japanese Society for the Promotion of Science JSPS.

9 ^b Assistant Professor.

10 ^c Professor and Director.

11 * Corresponding author; e-mail: olmati@t-kougei.ac.jp, pierluigi.olmati@gmail.com

13 **Abstract**

14 Design of blast loaded structures is usually carried out following a deterministic rather than
15 a probabilistic approach. The design load scenario would cover the plausible load
16 conditions (typically some conservative estimate) that a structure would experience if an
17 explosion occurs but the probability that the structure will satisfy the design performances
18 for the considered scenario remains unknown. Applying a performance-based design
19 framework typically requires arduous Monte Carlo simulations, but a probabilistic design
20 could also be achieved by a single structural analysis when consistent safety factors are
21 applied to the load and the structural resistance. Such a factor is proposed herein for the
22 case of components subjected to impulsive blast loads. The dependence of the safety factor
23 on the amount of explosive, stand-off distance and their variability is estimated numerically

1 and provided by means of regression formulas. A design example using the proposed safety
2 factor is carried out and Monte Carlo simulation is used for verification. The results
3 confirm the validity of the proposed safety factor approach and its applicability for the
4 performance-based design of blast loaded structures using the current design practice
5 methods.

6

7 **Keywords:** performance-based design; probabilistic analysis; safety factor; blast design;
8 terroristic explosions; blast load; vehicle borne improvised explosive devices.

9

Nomenclature

Latin upper case

A : loaded area of the element

APE : acceptable probability of exceedance

COV: coefficient of variation

K_{APE} : standard normal variate corresponding to non-exceedance probability of $1-APE$

K_{LM} : load-mass transformation factor

M : total mass of the element

M_v : number of values of the design parameters

N_p : number of design parameters

$P(\Theta > \theta | i)$: fragility curve

$P(\Theta > \theta | p, i)$: fragility surface

P_o : a value of the probability of exceedance of the limit state

PDF: probability density function

R : stand-off distance

RC: reinforced concrete

\bar{R} : mean value of the stand-off distance

SDOF: single degree of freedom

S_y : yield resistance

VBIED: vehicle borne improvised explosive device

V_R : stand-off distance variability

V_W : amount of explosive variability

Variability: coefficient of variation

W : amount of explosive

\bar{W} : mean value of the amount of explosive

Z : scaled distance

Latin lower case

d_y : yield displacement

i : impulse

\hat{i}_C : median value of the impulse capacity

\hat{i}_D : median value of the impulse demand

$i_D^{\bar{R}, \bar{W}}$: impulse demand calculated using \bar{W} and \bar{R} (deterministic impulse demand)

p : pressure

p_r : peak pressure

t_d : time duration of the triangular blast load

t_{d_d} : design time duration of the triangular blast load

V_{i_C} : impulse capacity variability

V_{i_D} : impulse demand variability

$y_{limit\ state}$: deflection of the limit state

y_{max} : maximum deflection

Greek upper case

Φ : cumulative distribution function of the standard normal distribution

Φ^{-1} : inverse of Φ

Θ : structural response parameter for the demand (load)

Greek lower case

α : see Equation (7)

λ : safety factor

ρ : percentage of reinforcements

θ : structural response parameter for the capacity (resistance) that defines the limit state of the structural element

$\lambda \cdot \hat{i}_D$: design impulse demand

1 Introduction

2 Design of a structural component loaded by a blast load is generally carried out following a
3 deterministic rather than a probabilistic approach (Stewart et al. 2012). The design load
4 scenario would represent the plausible load conditions that a component would experience
5 but the probability that the structure will satisfy the design performances for the considered
6 scenario remains unknown. Therefore, the reliability of blast resistant structures under
7 current design practices remains vague.

8 Generally a probabilistic design framework for blast loaded structures is investigated in
9 several research works that can be useful to understand both probabilistic models and
10 uncertainties affecting the design of blast resistant structures. Low and Hao (2001) carried
11 out a parametric investigation to establish appropriate probabilistic distributions of
12 resistance parameters for blast loaded structures. Netherton and Stewart (2009) and Stewart
13 and Netherton (2015) investigated the accuracy of the blast loading prediction models.
14 Chang and Young (2010) estimated the probability of failure for windows subjected to blast
15 loads. Shi and Stewart (2015a) calculated the probability of damage of RC columns subject
16 to explosive blast loading.

17 The current design trend for blast loaded structures is to use a single-degree-of-freedom
18 (SDOF) model approximation (Biggs 1964; Stochino 2014) for a pre-design and then carry
19 out detailed finite element simulations of the full multi-degree-of-freedom (MDOF) model
20 to verify/improve the initially achieved design by accurately assessing the structural
21 response (Nickerson et al. 2015). Monte Carlo simulations could be employed at both

1 design stages to estimate the reliability of the structure; however the computational
2 requirements are often prohibitive. The analysis of finite element models via Monte Carlo
3 simulation is simply impractical for design practice due to the complexity of a multi-
4 parameter finite element model, and the computer resources required for executing the
5 numerous simulations. The design itself is an iterative process, thus employing Monte
6 Carlo simulations remains complex even with SDOF models at the pre-design phase.

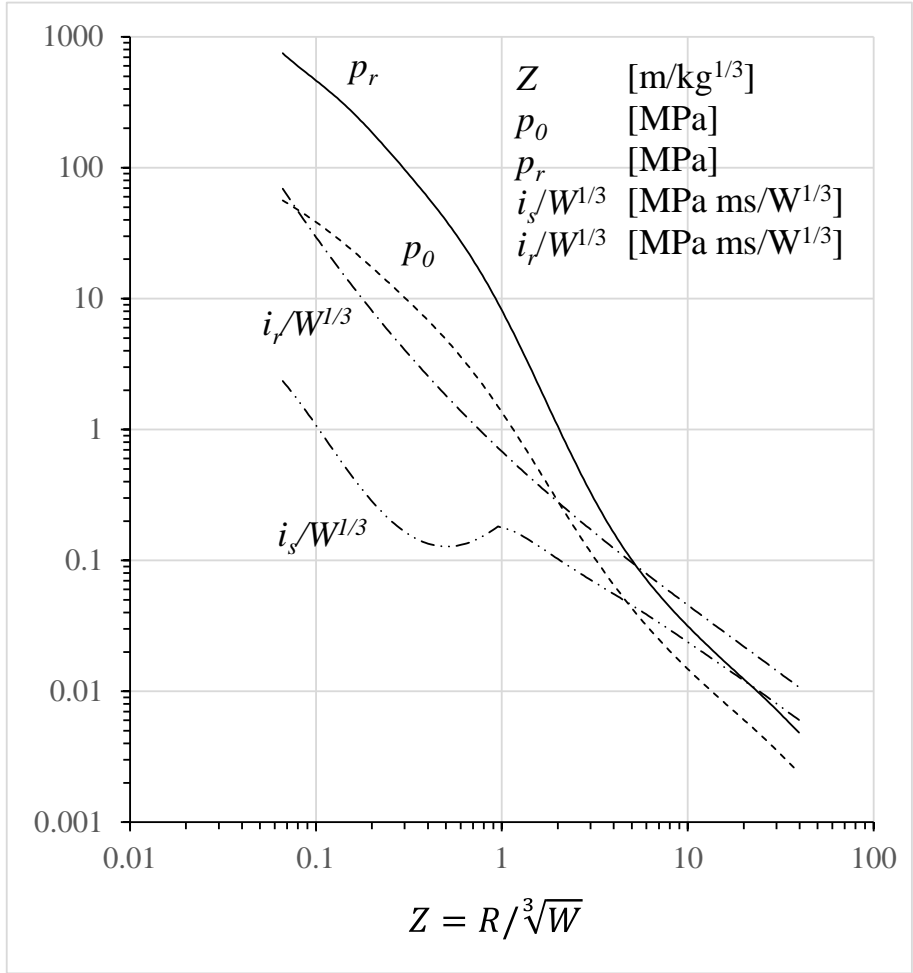
7 A simpler approach to accomplish a probabilistically consistent design of blast resistant
8 structures is the adoption of an appropriate safety factor format (Olmati et al. 2014, 2016)
9 similar to the LRFD (Load and Resistance Factor Design) approach (AISC 2003). This can
10 be calibrated to provide the desired acceptable probability of exceedance (*APE*) for any
11 structural performance target without expending human and computational resources or
12 deviating from the current state of practice. Herein, practice-oriented expressions are
13 provided for such a safety factor to derive a probabilistically-consistent design load for
14 structures subjected to impulsive blast where the probability density function of both
15 amount of explosive and stand-off distance are log-normally distributed. Therefore the
16 applicability of the proposed safety factor is limited to scenarios where both amount of
17 explosive and stand-off distance are lognormally distributed; other probability density
18 functions (e.g. uniform or normal) can be considered as well and the safety factor derived
19 in a similar manner as presented for lognormally distributed amount of explosive and stand-
20 off distance.

1 To validate the proposed approach the design of a reinforced concrete RC panel is carried
2 out using SDOF analyses and applying the safety factor to the blast load in order to achieve
3 10% probability of moderate component damage (US Army 2008). Successively, the
4 design, carried out using the proposed safety factor, is verified by performing a Monte
5 Carlo simulation, while a sensitivity analysis is also conducted. However a designer must
6 check the applicability of the proposed safety factor to the actual case and verify that other
7 indirect loads on the component as e.g. impact of debris could be negligible or add the
8 additional loads to the design blast load calculated using the proposed safety factor.

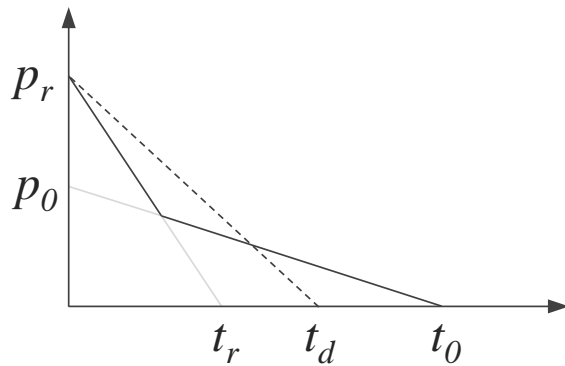
9 **2 Blast load model**

10 The blast load can be modelled as an equivalent triangular pulse as described in DoD
11 (2008). This equivalent pulse is calculated using empirical equations based on the scaled
12 distance Z which is the stand-off distance divided per the cube root of the amount of
13 explosive. The proposed safety factor is calculated using this blast load model, which is the
14 most popular among blast-design engineers. Furthermore a hemispherical surface burst
15 explosion is employed to represent a Vehicle-Borne Improvised Explosive Device VBIED
16 scenario. Figure 1 shows the blast load parameters where R is the stand-off distance, Z is
17 the scaled distance, W is the mass of explosive, p_0 and p_r are respectively the side-on and
18 reflected peak pressure, i_s and i_r are respectively the side-on and reflected impulse.

19



(a)



(b)

Figure 1: Blast load parameters according to DoD (2008): (a) Functional relationship with respect to the scaled distance, and (b) definition of the equivalent triangular pulse.

1

2 The equivalent triangular blast load is characterized by the peak pressure p_r and impulse i ,
3 therefore the duration of the equivalent triangular pulse t_d is equal to twice the impulse i
4 divided the peak pressure p_r (a decay pressure coefficient could be also defined as in
5 Gantes and Pnevmatikos (2004)). The blast load model is considered deterministic given R
6 and W , so its uncertainty is usually determined by propagating the uncertainty in the two
7 parameters. Additional uncertainty can be included, e.g., in the form of the blast model
8 error, an exhaustive assessment of which can be found in Stewart and Netherton (2015).

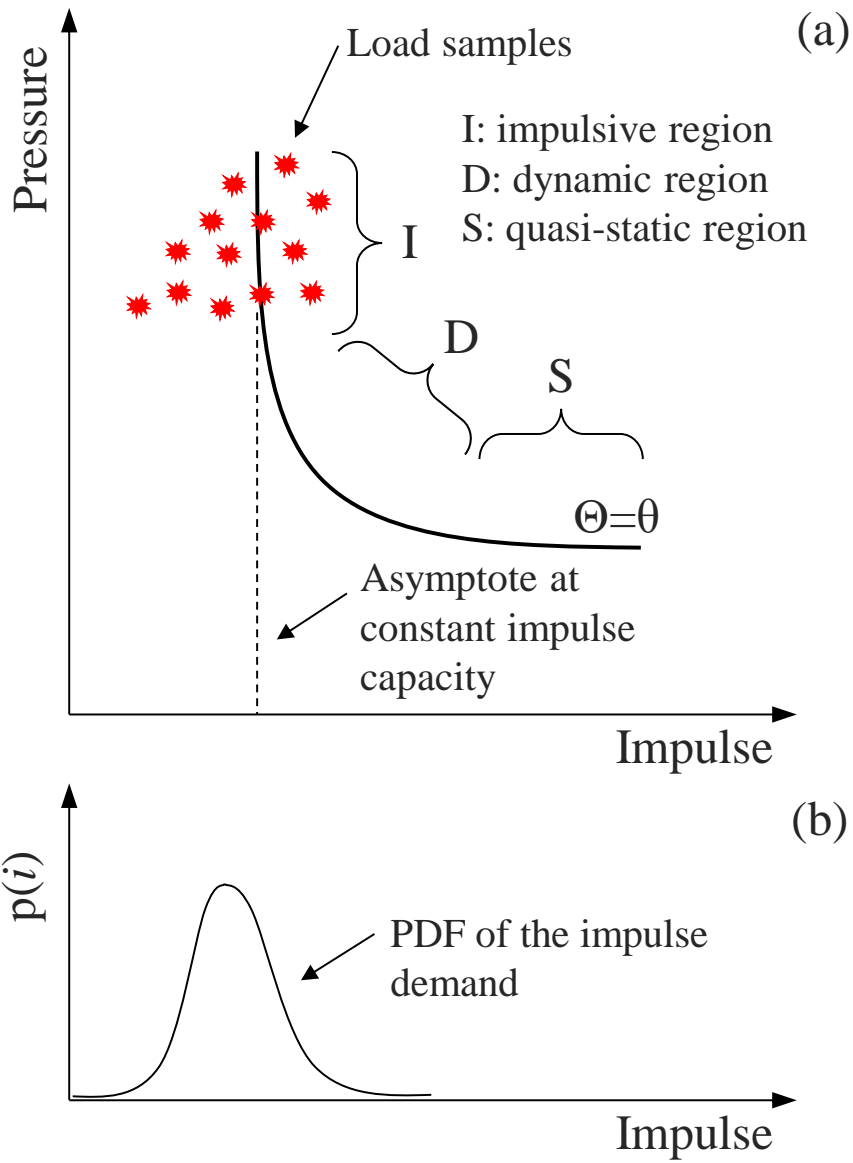
9 **3 Structures subjected to blast loads**

10 The structural response θ of a blast-loaded structural element can be represented on the
11 pressure–impulse diagram that is developed by considering all the pairs of pressure and
12 impulse demand for which the element responds with the selected structural response θ ; see
13 for example Krauthammer et al. (2008), Shi et al. (2008) and Parisi et al. (2016). Therefore
14 the contours of the pressure–impulse diagram represent the behavior of the structural
15 element under all the possible blast loading conditions. The structural response θ of a blast
16 loaded structure can be the middle span deflection or, as considered in this study, the
17 support rotation (US Army 2008; DoD 2008). Both middle span deflection and support
18 rotation are good response parameters θ when the element assumes a flexural governed
19 deflection shape. This is valid, as described in both US Army 2008 and DoD 2008, if there

1 is not too much variation, approximately less than 25%, in the blast load over the middle
2 two-thirds of the component span length which typically occurs for a scaled standoff
3 distance Z greater than approximately 1.2 to $2.0 \text{ m/kg}^{1/3}$ (3.0 to $5.0 \text{ ft/lb}^{1/3}$).

4 As shown in Olmati et al. (2014, 2016), for a given structural response parameter θ , there is
5 an infinite number of such pressure–impulse diagrams each one corresponding to a single
6 value of the probability of exceedance of the given structural response θ . If we consider the,
7 so-called, fragility surface $P(\Theta > \theta | p, i)$ of the probability of the structural response θ
8 exceeding an arbitrary value of θ given pressure and impulse, then each pressure–impulse
9 diagram is a cross section of this surface with a plane at a constant probability of P_0 .

10 Figure 2(a) shows an example of a pressure–impulse diagram and its regions: “I” the
11 impulsive region where only the impulse is relevant; “D” the dynamic region where the
12 structural response of the component is governed by the load shape and pressure
13 magnitude; and “S” the quasi-static region where only the peak pressure is relevant. Figure
14 2(b) shows the Probability Density Function PDF of the impulse demand generated from
15 the blast load samples. If the blast loads samples are in the impulsive region of the
16 pressure–impulse diagram the structural response depends from the blast impulse only.



1

2 Figure 2: (a) example of pressure–impulse diagram and load samples; (b) example of
3 probability density function of the impulse demand (load).

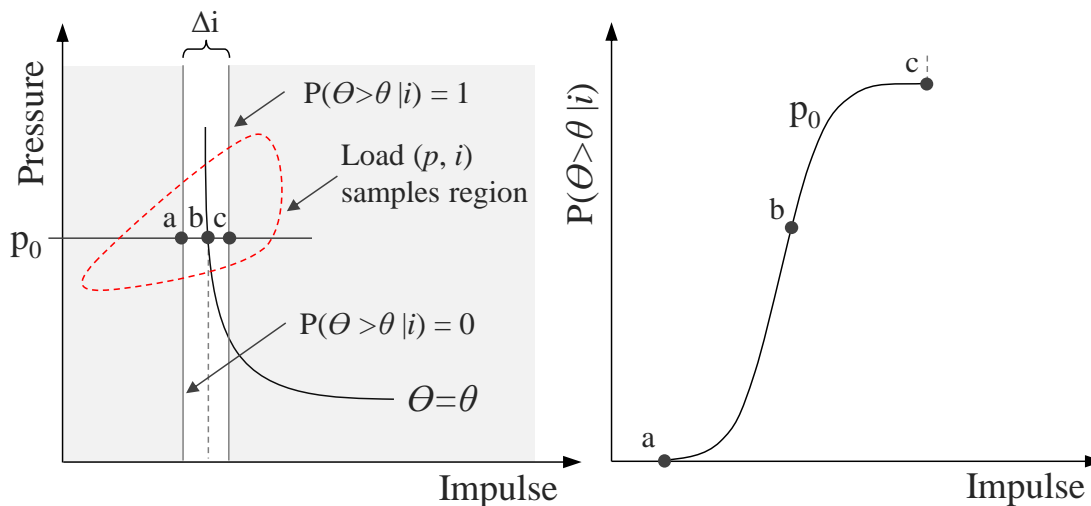
4

- 1 The maximum response y_{max} of an element loaded in the impulsive region of the pressure–
- 2 impulse diagram could be calculated with the approximate formula shown in Equation (1).
- 3 The peak pressure does not affect the equation, only the impulse matters.

$$4 \quad y_{max}(i) = \frac{1}{2} \left(\frac{(iA)^2}{(K_{LM} M) S_y} + d_y \right) \quad (1)$$

- 5 A (mm^2) is the loaded area of the element, i ($\text{MPa}\cdot\text{s}$) is the impulse demand, M (tonne) is
- 6 the total mass of the element, S_y (N) and d_y (mm) are the yield resistance and displacement,
- 7 respectively, and K_{LM} is the load-mass transformation factor; see Krauthammer et al. (2008).
- 8 Equation (1) is not intended for carrying out the design but it is useful to report it here for
- 9 illustrative purposes.

- 10 Under the hypothesis of impulse sensitive structure the pressure–impulse diagram can be
- 11 approximated with its impulsive asymptote as shown in Figure 2(a) and Figure 3. Then the
- 12 fragility of such an element depends only on the impulse and it can be expressed as
- 13 $P(\Theta > \theta | i)$; see Figure 3.



14

1 Figure 3: Conceptual definition of fragility curve for impulse sensitive structures (Olmati et
2 al. 2016).

3 **4 Safety factor λ and design blast load**

4 The proposed safety factor λ is a scalar that when multiplied by the blast nominal value it
5 delivers the blast load that the structural element needs to withstand without exceeding the
6 threshold value of design response parameter θ associated with the limit-state of interest.

7 The safety factor λ is function of the acceptable probability of exceedance APE of the
8 design response parameter θ (limit state) and both the impulse demand (load) and capacity
9 (resistance) variability. If lognormality is adopted for both the impulse demand (as
10 suggested by Olmati et al. 2014, 2016) and the impulse capacity, then the safety factor λ
11 can be expressed in a format consistent with the work of Cornell (1969) and Cornell et al.
12 (2002) used in earthquake engineering:

$$13 \quad \lambda = e^{K_{APE} \cdot \sigma_T} < \hat{i}_C / \hat{i}_D \quad (2)$$

$$14 \quad \sigma_T = \sqrt{\ln(1 + V_{i_D}^2) + \ln(1 + V_{i_C}^2)} \quad (3)$$

$$15 \quad K_{APE} = \Phi^{-1}(1 - APE) \quad (4)$$

16 In Equations (2 – 4), \hat{i}_C and \hat{i}_D are the median values of the impulse capacity and demand,
17 respectively, while V_{i_C} and V_{i_D} are the corresponding coefficients of variation, Φ^{-1} is the
18 inverse of the cumulative distribution function of the standard normal distribution, and K_{APE}
19 is the standard normal variate corresponding to non-exceedance probability of $1 - APE$.

1 Figure 3 shows the fragility $P(\Theta \geq \theta | i)$ of a structural element subjected to impulsive blast
 2 loads. To calculate the safety factor λ a fragility analysis of the element subjected to
 3 impulsive blast loads should be carried out (Olmati et al. 2014, 2016). For most cases,
 4 though, the uncertainties of the component, and most prominently the variability of the
 5 impulse capacity V_{iC} , can be neglected because the variability of impulse demand, V_{iD} ,
 6 generally dominates Equation (3) (e.g. Shi and Stewart 2015b).

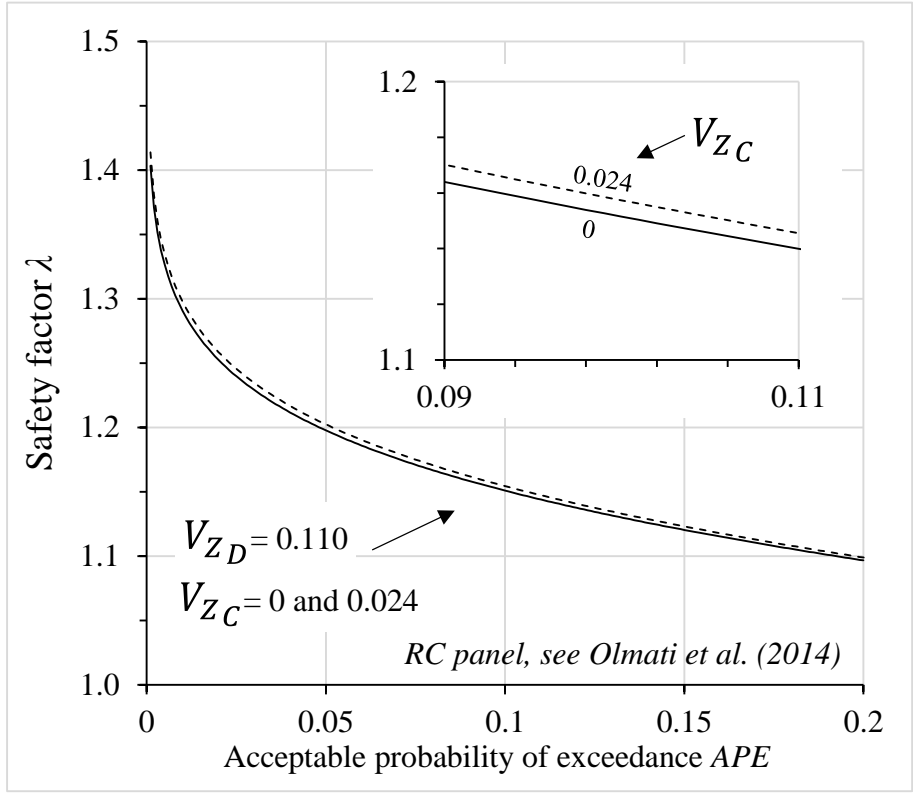
7 As an example, the fragility of a reinforced concrete RC panel and of a blast resistant door
 8 is calculated in Olmati et al. (2014, 2016) respectively. The variability of the capacity for
 9 both the cases of study is reported in Table 1 together with the variability of the demand for
 10 a specific limit state; for detailed information please refer to Olmati et al. (2014 and 2016).

11 Table 1: Variability of the demand and capacity for two building components (Olmati et al.
 12 2014, 2016). The fragility of the RC panel has been calculated using the scaled distance Z
 13 as loading parameter, a variable generally called intensity measure IM ; see e.g. Luco and
 14 Cornell (2000). Thus, in Equation (3) V_{iD} and V_{iC} are replaced by V_{ZD} and V_{ZC} respectively.

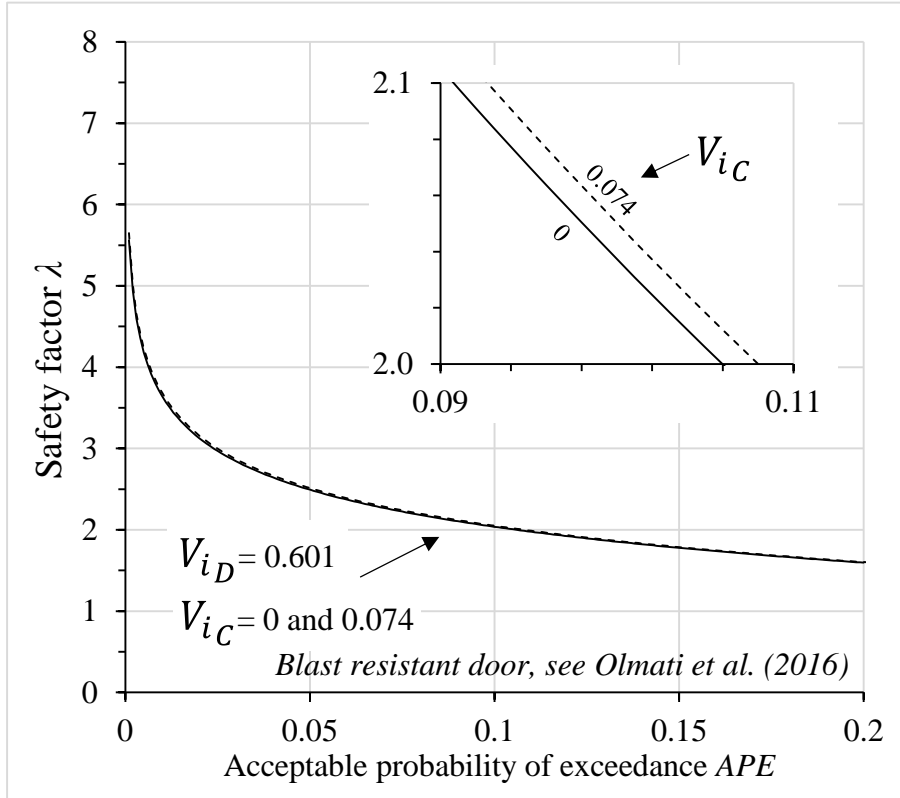
RC panel	Blast resistant door
(Moderate damage limit state)	(Operability limit state)
$V_{ZD} = 0.110$	$V_{iD} = 0.601$
$V_{ZC} = 0.024$	$V_{iC} = 0.074$

15 The impulse demand variability V_{iD} for the blast resistant door, due to accidental detonation
 16 of mortar rounds, is quite large because a uniform probability density function is used for

1 the stand-off distance; see Olmati et al. (2016). While the variability of the demand for the
2 reinforced concrete panel, due to a vehicle bomb attack, is smaller than the case of study of
3 the blast resistant door because of the presence of defensive measures: a fence perimeter is
4 present to prevent vehicles from accessing the protected area while access to trucks is
5 negated in the surrounding area (Olmati et al. 2014). It is important to consider as well that
6 the nonlinearity of the blast problem does not allow for a simple propagation of uncertainty.
7 Thus, a variability of the scaled distance of around 0.1 translates to a nearly double
8 variability for the peak pressure and impulse; see contextually Figure 1. In fact the impulse
9 demand variability V_{i_D} for this scenario is 0.22, i.e. more than twice the scaled distance
10 variability V_{Z_D} . Furthermore the variability of the capacity for the blast resistant door is
11 predominantly due to the epistemic uncertainties of the equivalent SDOF. While the
12 variability of the capacity for the reinforced concrete panel is due to the material resistance
13 uncertainties. The safety factor λ obtained from Equation (3) is plotted in Figure 4 for the
14 components shown in Table 1.



(a)



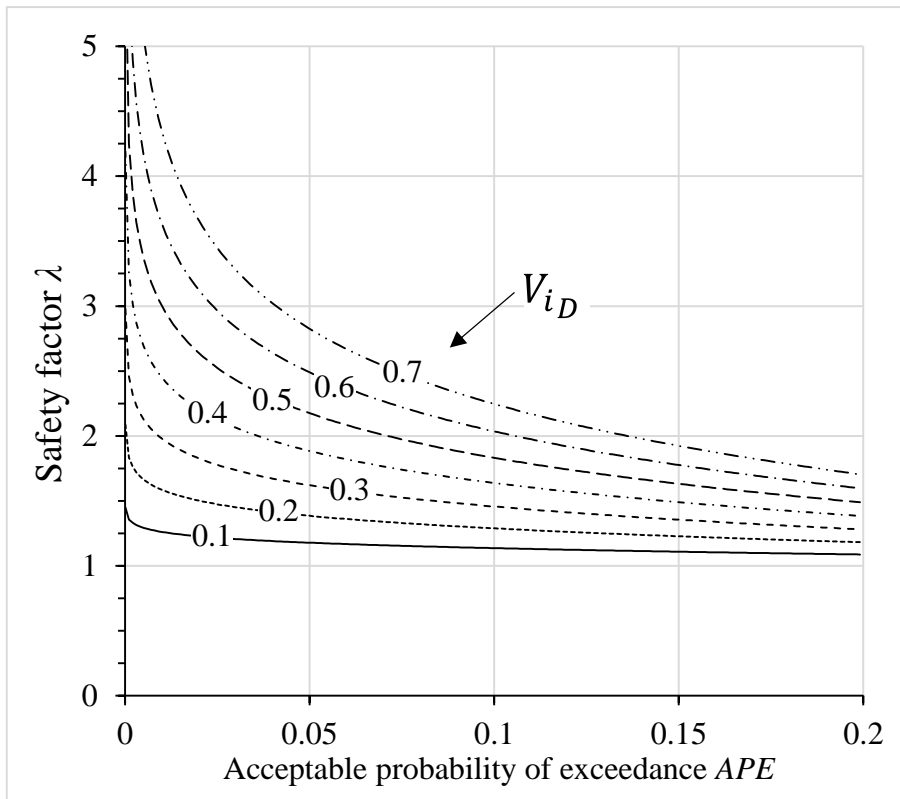
(b)

Figure 4: Plot of the safety factor versus the *APE* for two components, (a) an RC panel, and (b) a blast resistant door. For both RC panel and blast resistant door the case where structural uncertainties are included is also shown for comparison purposes.

1

2 It is evident from Figure 4 that the structural uncertainties of an element subjected to
 3 impulsive blast loads can be neglected if the variability of the demand is greater enough
 4 than the variability of the capacity. In this case the variability of the demand determines the
 5 value of the safety factor λ ; see Equation (3). However Olmati et al. (2016) shows a method
 6 to assess the uncertainties of the structure which are described, in this case, by the

1 variability of the impulse capacity V_{iC} . If the variability of the impulse capacity V_{iC} is
 2 neglected the fragility $P(\Theta \geq \theta | i)$ of the structural element is reduced to a constant function of
 3 the median value of the impulse capacity \hat{i}_C . As consequence the mean values of structural
 4 parameters can be used in the element structural model. Figure 5 shows the safety factor λ
 5 plotted for values of the impulse demand variability V_{iD} spanning from 0.1 to 0.7; the value
 6 of the safety factor λ for a specific acceptable probability of exceedance APE of the
 7 structural performance (limit state) can be selected directly from Figure 5. Useful
 8 fundamental criteria for choosing an opportune probability of exceedance APE can be
 9 found in Stewart (2008, 2010, 2011 and 2012).



10

11 Figure 5: The safety factor λ as a function of V_{iD} spanning from 0.1 to 0.7.

1

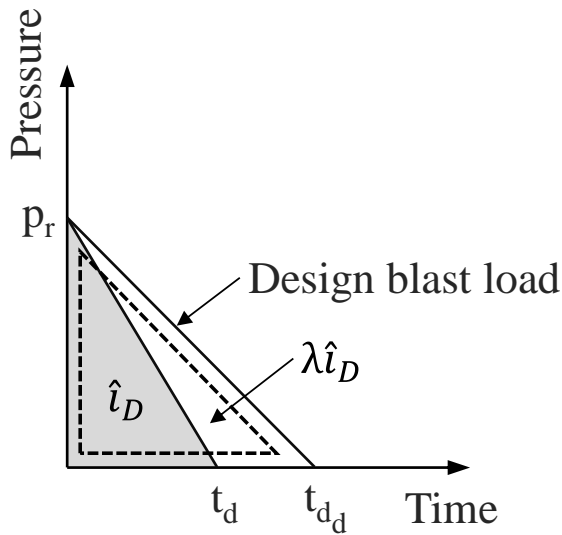
2 If Equation (1) is used as a mechanical model of the structural element subjected to
3 impulsive blast loads the safety factor λ is applied as follows:

4
$$y_{max}(\lambda \hat{i}_D) = \frac{1}{2} \left(\frac{(\lambda \hat{i}_D A)^2}{(K_{LM} M) S_y} + d_y \right) < y_{limit\ state} \quad (5)$$

5 However if an equivalent SDOF analysis or a finite element simulation is used instead, the
6 proposed safety factor λ applied by increasing the duration time t_d of the equivalent
7 triangular blast load.

8
$$t_{d_d} = 2\lambda \hat{i}_D / p_r \quad (6)$$

9 where t_{d_d} is the (increased) design duration time and p_r is the peak pressure of the design
10 blast load, graphically presented in Figure 6. Therefore the reliability of the structural
11 element subjected to impulsive blast loads is guaranteed by a design carried out using an
12 equivalent SDOF analysis or a finite element simulation where design blast load, defined
13 by p_r and t_{d_d} , is applied to the structural element.



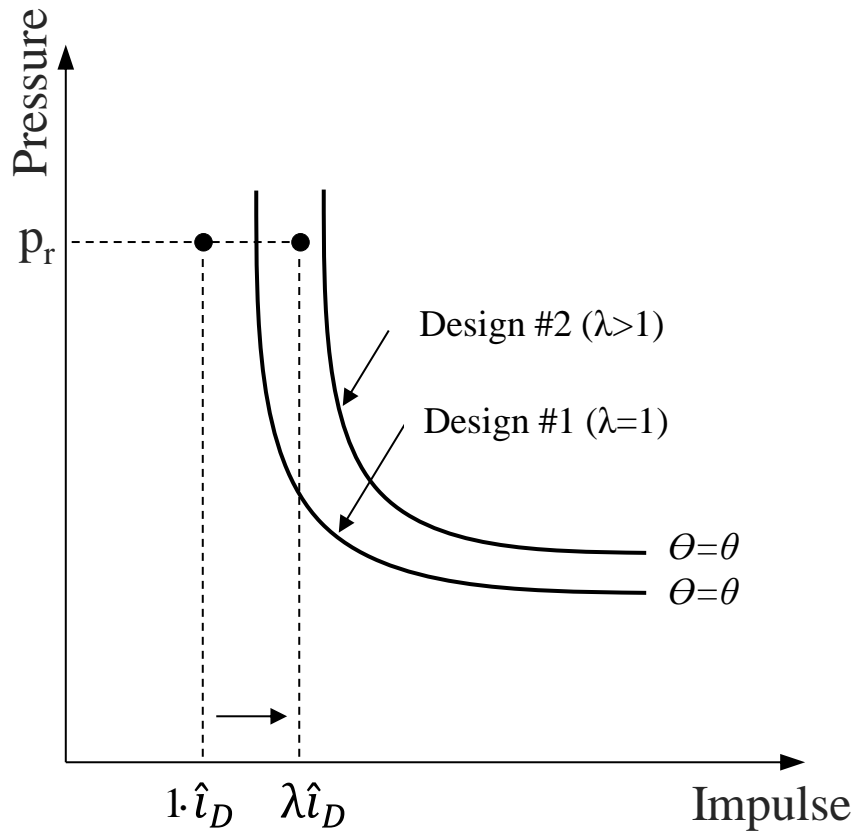
1

2 Figure 6: Design blast load; \hat{i}_D and $\lambda \hat{i}_D$ are respectively the median and design value of the
 3 impulse demand.

4

5 To understand the effect of applying the design blast load to a structural element, let us
 6 consider two such alternative designs for a given element, aptly named #1 and #2. Their
 7 performance is shown schematically in Figure 7 on the pressure–impulse diagram obtained
 8 using mean values of the element structural parameters. Design #1 can withstand the
 9 median value of the blast load but its reliability is unknown. In fact design #1 fails the
 10 verification when an acceptable probability of exceedance APE of the limit-state threshold
 11 θ is selected and the correspondent safety factor λ is applied to the blast load. While design
 12 #2 satisfies the selected APE . Vice versa if the design is based on the worst case scenario
 13 the design outcome could be irrationally oversized because the resulting probability of
 14 exceedance of the limit-state threshold θ could be much smaller than the mandated APE

- 1 defined in a performance-based design perspective. Therefore a risk-based design is
- 2 necessary wherever uncertainty exists, as in the case of blast-resistant structures.



- 3
- 4 Figure 7: Pressure–impulse diagram and the design blast load for two conceptual design
- 5 cases. Design #1 does not incorporate the effect of uncertainty ($\lambda = 1$). Design #2 is
- 6 designed to a higher standard ($\lambda > 1$), thus it can withstand higher loads for the same limit
- 7 state expressed by the threshold θ and satisfy *APE*.

8

- 9 To calculate the median value of the impulse demand \hat{i}_D and its variability V_{i_D} , Monte
- 10 Carlo simulation is generally needed. However, based on Monte Carlo simulation, the

1 relationships giving the median impulse demand \hat{t}_D and its variability V_{i_D} can be estimated
2 to become functions of the mean values of the stand-off distance \bar{R} and amount of
3 explosive \bar{W} and their coefficients of variation V_R and V_W .

4 **5 Impulse demand**

5 The considered blast load scenario is a terrorist attack made by VBIED, which is a surface
6 burst explosion (Stewart and Mueller 2014, Yokohama et al. 2015, Grant and Stewart
7 2015). This scenario is characterized by a mean value of the amount of explosive \bar{W} (here
8 intended as TNT equivalent explosive) placed into a vehicle located at a mean value of the
9 stand-off distance \bar{R} where the detonation occurs. The stand-off distance is achieved by a
10 defense perimeter generally made by a fence or bollards installed around the structure to be
11 protected (FEMA 2015).

12 Generally the variability of the amount of explosive V_W is due to many uncertainties. The
13 explosive quantity that an attacker is able to fit in a vehicle is of course a source of
14 uncertainty but also the type of the explosive, described by TNT equivalent factor (NEQ),
15 gives a consistent contribution to the overall amount of explosive variability V_W .
16 Furthermore the accuracy of the blast load model (see Fig. 1) is a source of uncertainty as
17 well that could be quantified and pertinently included in the amount of explosive variability
18 V_W . Therefore the amount of explosive variability V_W is an overall estimation of all the
19 uncertainties affecting the blast load model and the amount of explosive. Further
20 information on blast load model error and other sources of variability can be found in
21 Stewart and Netherton (2015). The stand-off distance variability V_R is due to the

1 uncertainties on the detonation distance from the target. Generally a VBIED would be
2 placed at the minimum stand-off distance delimited by the defense perimeter; however this
3 perimeter could be violated or the vehicle could not be placed for some reason just beside
4 the defense perimeter. Data about the mean values of amount of explosive \bar{W} and stand-off
5 distance \bar{R} together with their variability V_W and V_R may be defined in accordance with
6 local government, security agencies and pertinent authorities.

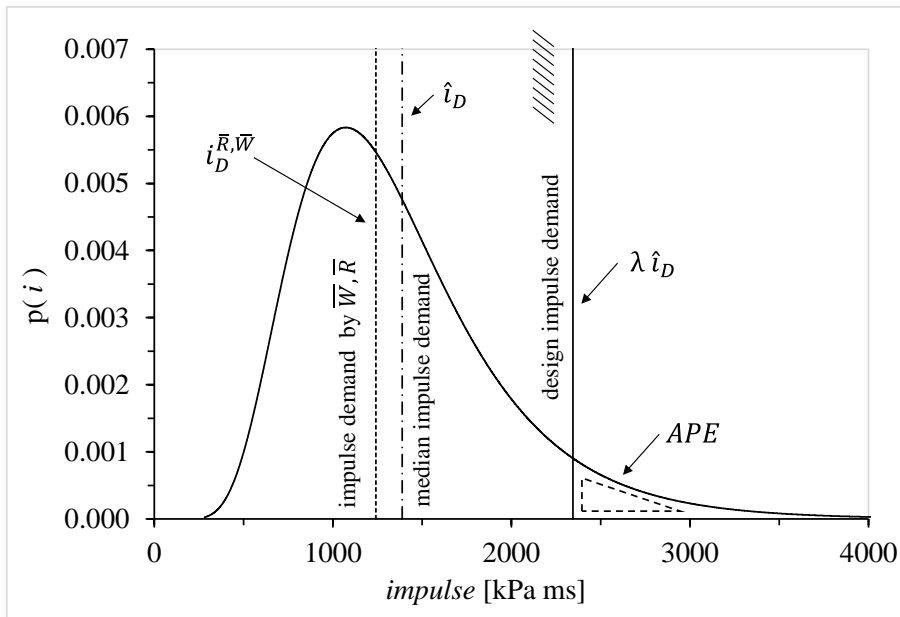
7 As shown in Section 4 the median value of the impulse demand \hat{i}_D is required in order to
8 use the safety factor λ in the design. The relationship of the median value of the impulse
9 demand \hat{i}_D vis-a-vis the impulse demand $i_D^{\bar{R},\bar{W}}$ that is calculated by assuming mean value of
10 the amount of explosive \bar{W} and stand-off distance \bar{R} is generally unknown. A
11 dimensionless coefficient α is here defined as the ratio between the median value of the
12 impulse demand \hat{i}_D and the impulse demand $i_D^{\bar{R},\bar{W}}$. Coefficient α is calculated in Section 5.1
13 while the impulse demand variability V_{i_D} to use in Equation (5) is discussed in Section 5.2.
14 For both coefficient α and impulse demand variability V_{i_D} the dependence from the mean
15 value of the amount of explosive \bar{W} can be neglected; see Section 5.1 and 5.2. Thus, we
16 may represent their definitions as:

$$17 \quad \hat{i}_D = \alpha(V_W, V_R, \bar{R}) \cdot i_D^{\bar{R},\bar{W}} \quad (7)$$

$$18 \quad V_{i_D} = V_{i_D}(V_W, V_R, \bar{R}) \quad (8)$$

19 Figure 8 shows the probability density function of the impulse demand obtained for the
20 case study and validation presented in Section 7. On this plot one can better understand the

1 relationship between the impulse demand $i_D^{\bar{R}, \bar{W}}$ obtained from the mean value of the amount
 2 of explosive \bar{W} and stand-off distance \bar{R} , the median value of the impulse demand \hat{i}_D , the
 3 design impulse demand $\lambda \hat{i}_D$ and the acceptable probability of exceedance APE of the limit
 4 state. A valid design of a structural element that ensures the desired APE of the structural
 5 performance (limit state) must provide an impulse capacity greater than the design impulse
 6 demand $\lambda \hat{i}_D$ as shown in Figure 8.



7
 8 Figure 8: PDF $p(i)$ of the impulse demand, together with the impulse values corresponding
 9 to: the impulse demand $i_D^{\bar{R}, \bar{W}}$, the median of the impulse demand \hat{i}_D and the factored design
 10 impulse demand $\lambda \hat{i}_D$ for the case study.

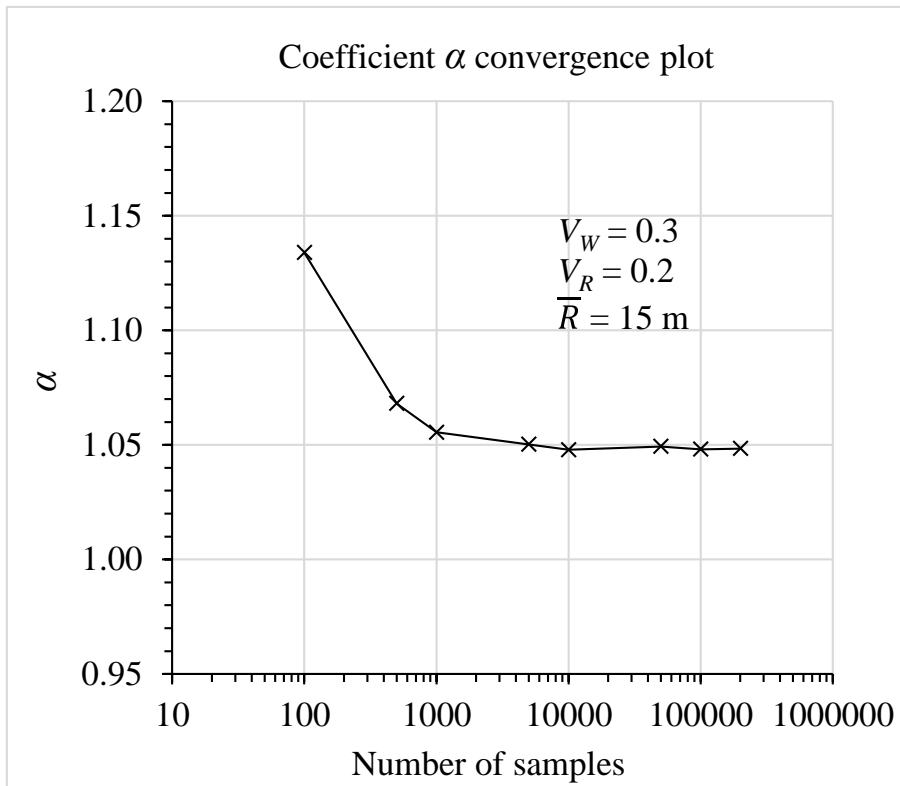
11

1 In the following, coefficient α and impulse demand variability V_{i_D} are provided for
 2 variability of explosive mass V_W and stand-off distance V_R ranging from 0.0 to 0.5, while a
 3 range of 5 to 30 meters of the mean stand-off distance \bar{R} is considered.

4

5 **5.1 Coefficient α**

6 Coefficient α multiplies the value of the impulse demand $i_D^{\bar{R}, \bar{W}}$ in order to estimate the
 7 median value of the impulse demand \hat{i}_D ; see Equation (7). A closed-form solution for
 8 coefficient α is not available, thus Monte Carlo simulations is used to calculate it
 9 numerically. 100,000 samples are used to ensure accuracy of outputs; Figure 9 shows the
 10 convergence plot of coefficient α .



11

1 Figure 9: Monte Carlo simulation convergence plot of coefficient α .

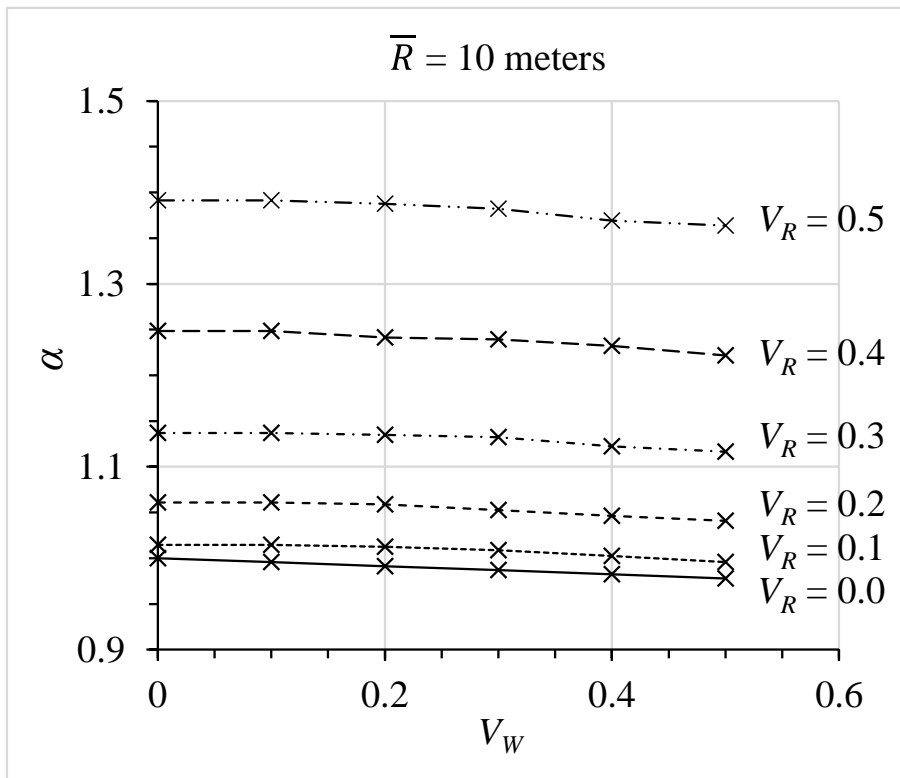
2

3 Coefficient α , is provided as a function of V_W , V_R and \bar{R} by means of a regression formula
 4 which is affected by a maximum absolute error of 1.8% calculated over the fitted range.

5
$$\alpha = 1 + (19.5 - 17.9 \cdot \bar{R}^{0.012}) \cdot (1.5 \cdot V_R^2 - 0.06 \cdot V_R \cdot V_W - 0.03 \cdot V_R - 0.04 \cdot V_W) \quad (9)$$

6 for $V_R \leq 0.5, V_W \leq 0.5$ and $5 \text{ m} \leq \bar{R} \leq 30 \text{ m}$

7 Note that α is insensitive to mean mass of explosive \bar{W} . Figure 10 shows a typical chart of
 8 coefficient α as function of V_W , V_R and for $\bar{R}=10 \text{ m}$.



9

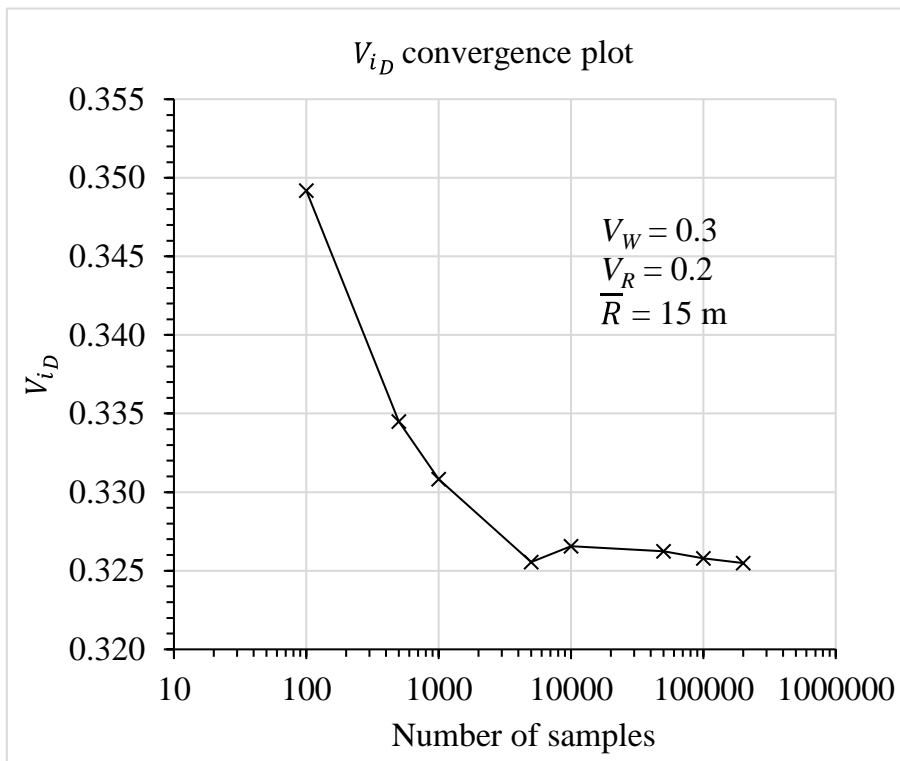
10 Figure 10: Plot of coefficient α as function of V_W , V_R for $\bar{R}=10 \text{ meters}$.

1

2 Coefficient α has a stronger dependence on the stand-off distance variability V_R rather than
 3 the amount of explosive variability V_W . This is in line with the fact that the blast pressure
 4 decreases with the cubic of the distance from the blast source to the target while the amount
 5 of explosive is under the cube root in defining the scaled distance and impulse; see Figure 1.

6 **5.2 Variability of the impulse demand V_{i_D}**

7 Monte Carlo simulations are used as well to calculate the values of the impulse demand
 8 variability V_{i_D} as a function of V_W , V_R and \bar{R} . Also for computing the variability of the
 9 impulse demand V_{i_D} 100,000 samples are used to ensure accuracy of outputs; Figure 8
 10 shows the convergence plot.



11

1 Figure 11: Monte Carlo simulation convergence plot of the impulse demand variability V_{iD} .

2

3 The impulse demand variability V_{iD} is provided by means of a regression formula shown in

4 Equation (10) which is affected by a maximum absolute error of 10.8% calculated over the

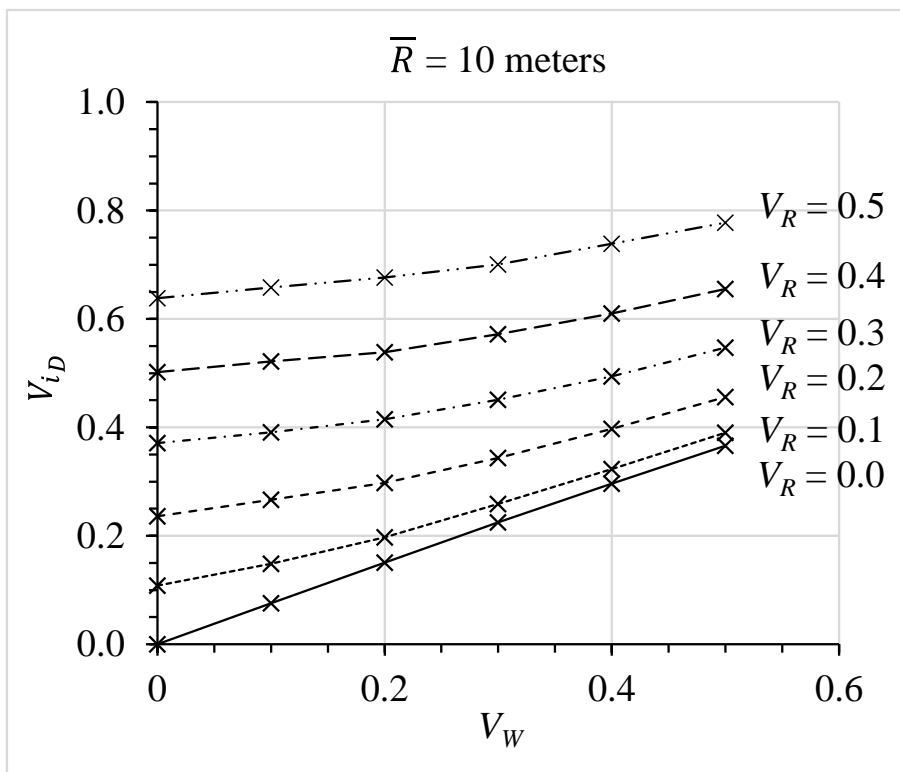
5 fitted range.

6
$$V_{iD} = (1.074 - 0.004 \cdot \bar{R}) \cdot (0.84 \cdot V_R + 0.63 \cdot V_W - 0.69 \cdot V_W \cdot V_R) + (0.54 + 3.13 \cdot \bar{R}^{-1.09}) \cdot V_R^2 \quad (10)$$

7 for $V_R \leq 0.5, V_W \leq 0.5$ and $5 \text{ m} \leq \bar{R} \leq 30 \text{ m}$

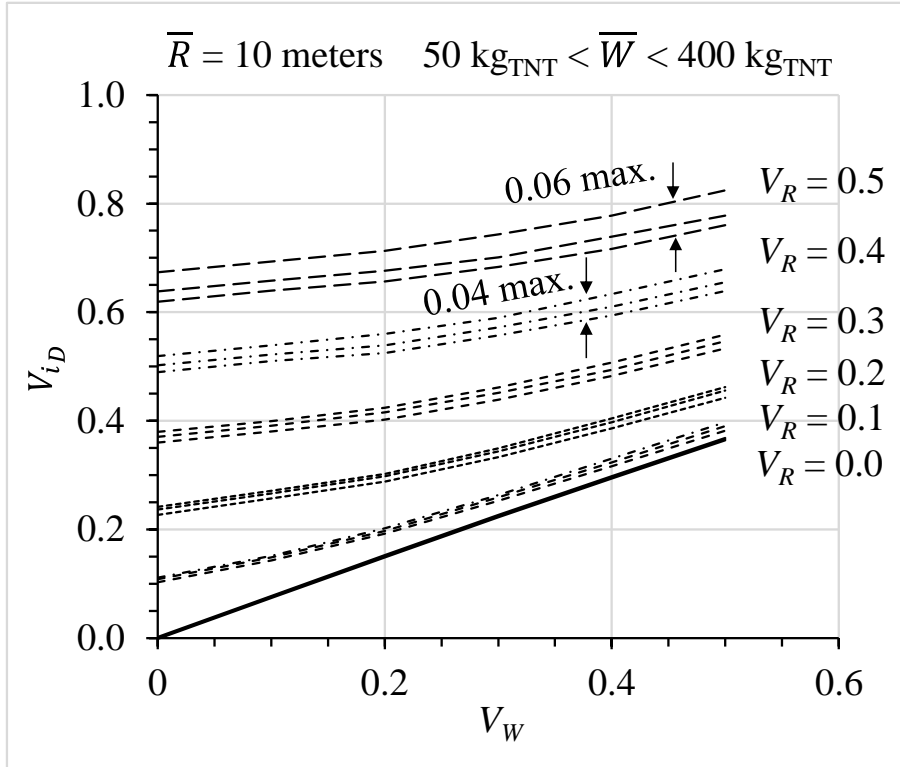
8 For illustrative purposes the impulse demand variability V_{iD} function of V_W, V_R and $\bar{R}=10$

9 meters is shown in Figure 12.



10

1 Figure 12: Plot of impulse demand variability V_{i_D} as function of V_W , V_R and $\bar{R}=10$ meters.
2
3 The variability of the impulse demand V_{i_D} is strongly dependent on the variability of both
4 amount of explosive V_W and stand-off distance V_R as shown in Figure 12, whereas
5 coefficient α is mainly dependent on the variability of the stand-off distance V_R only. Also
6 for the impulse demand variability V_{i_D} the dependence from the mean value of the amount
7 of explosive \bar{W} can be neglected as shown in Figure 13 because the maximum difference of
8 the impulse demand variability V_{i_D} calculated for \bar{W} from 50 to 400 kg_{TNT} is 0.06 and it
9 occurs when the stand-off distance variability is $V_R=0.5$. Therefore the maximum error in
10 estimating the safety factor λ using Equation (2) is only 5% when the stand-off variability is
11 0.5.



1

2 Figure 13: Impulse demand variability V_{iD} calculated for $\bar{R}=10$ meters and $\bar{W} = 50, 100$ and
 3 $400 \text{ kg}_{\text{TNT}}$. The effect of \bar{W} is small enough to be neglected.

4 **6 Design Procedure**

5 The procedure for using the proposed safety factor λ in the design of elements subjected to
 6 impulsive blast loads is summarized as the following:

- 7 1) Determine the mean value of both amount of explosive \bar{W} and stand-off distance \bar{R} .
- 8 2) Determine the variability of mass of explosive V_W and stand-off distance V_R .
- 9 3) Choose the acceptable probability of exceedance APE of the limit state.

1 These inputs are provided in accordance with local government and pertinent authorities;
2 both the mean value and variability of the amount of explosive and stand-off distance are
3 also dependent on the adopted security measures. The uncertainties affecting the structure
4 are not assessed, as explained in Section 4, therefore the impulse capacity variability V_{i_C} is
5 taken to be zero.

6 4) Calculate the impulse demand $i_D^{\bar{R}, \bar{W}}$ and peak pressure p_r using the mean value of the
7 amount of explosive \bar{W} and stand-off distance \bar{R} ; Figure 1 can be used.

8 5) Obtain coefficient α using Equation (9).

9 6) Calculate the median value of the impulse demand \hat{i}_D using Equation (7).

10 7) Obtain the variability of the impulse demand V_{i_D} using Equation (10).

11 8) Calculate the safety factor λ using Equation (2) or the chart provided in Figure 5
12 ($V_{i_C}=0$).

13 9) Apply the safety factor λ to the blast load by increasing the duration time of the
14 blast pulse as shown in Equation (6).

15 10) Perform a structural analysis using the reliability-based design load.

16 11) Check if the structural response parameter θ exceeds the limit state threshold and
17 iterate the design until the limit state is satisfied.

1 These steps are applied in the next section in order to design a RC panel subjected to
2 impulsive blast loads. Then a Monte Carlo simulation is carried out to check if the actual
3 design respects the selected acceptable probability of exceedance *APE* of the limit state.

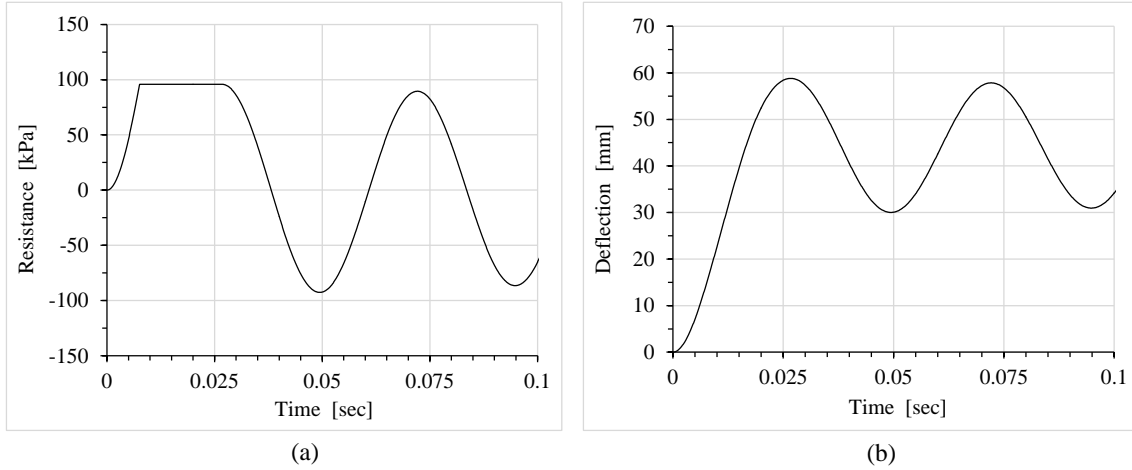
4 **7 Application and validation**

5 The RC panel, simply supported at its extremities, is 3500 mm long, 1500 mm wide and
6 200 mm thick. It is reinforced both sides and the longitudinal reinforcement cover is 35 mm.
7 The reinforcing steel mean strength is 495 MPa while the concrete mean strength is 28 MPa.
8 The structural analysis is carried out using an equivalent single degree of freedom SDOF
9 model, since the scaled distances *Z* considered in this applications are greater than
10 approximately 1.2 to 2.0 m/kg^{1/3} (3.0 to 5.0 ft/lb^{1/3}), following a widely used design
11 procedure; see US Army (2008). An equivalent SDOF model of a structural component is
12 made by developing appropriate transformation factors for the system's mass, damping,
13 load and resistance. Inherent to a SDOF analysis is the assumption that the system behaves
14 only in a single deflected shape. As the system begins to deflect under the blast load it
15 eventually yields and forms plastic hinges at various locations depending on the applied
16 boundary conditions. Therefore, the transformation factors are adjusted accordingly to
17 account for the change in deflected shape. For a simply supported RC panel it is assumed
18 that a single plastic hinge forms at mid-span of the panel thus the resistance-deflection
19 relationship for such a panel is assumed elastic-perfectly plastic.

20 In the following the probabilistic design of the reinforced concrete panel subjected to a
21 VBIED explosion is carried out as described in the design procedure:

- 1 - Step (1) and (2): mean value of the stand-off distance \bar{R} and its variability V_R are
2 taken equal to 20 meters and 0.3 respectively. The mean amount of explosive \bar{W} is
3 227 kg_{TNT} and its variability V_W is equal to 0.3. This corresponds to a car sized (500
4 lb) VBIED (FEMA 2005). These stochastic parameters are considered here as an
5 example to show the application of the safety factor λ . In a real scenario these
6 stochastic parameters are calculated pertinently to the design case considering the
7 security measures in place to prevent unacceptable situations. For example defense
8 measures can be placed in order to keep trucks traffic away from a sensible target
9 while only cars access is allowed. The mean value of amount of explosive \bar{W} and
10 stand-off distance \bar{R} and their variability V_W and V_R will represent this situation.
- 11 - Step (3): moderate damage of the RC panel is considered as the limit state (US
12 Army 2008). This means that for a non-load bearing RC panel the maximum
13 support rotation should not exceed 2 degrees which corresponds to a middle span
14 deflection equal to 60 mm. As an illustrative application, the acceptable probability
15 of exceedance APE of the moderate damage limit state is taken as 10%.
- 16 - Step (4): maximum peak pressure p_r and impulse demand $i_D^{\bar{R},\bar{W}}$ are 261 kPa and
17 1240 kPa·ms respectively calculated using Figure 1 for $Z=3.278 \text{ m/kg}^{1/3}$.
- 18 - Step (5): α is 1.1 calculated using Equation (9).
- 19 - Step (6): median value of the impulse demand \hat{i}_D is $1.1 \cdot 1240 = 1364 \text{ kPa} \cdot \text{ms}$.

- 1 - Step (7): variability of the impulse demand V_{i_D} is 0.43 calculated using Equation
2 (10).
- 3 - Step (8): safety factor λ is 1.7 obtained by Equation (2) or Figure 5.
- 4 - Step (9): design duration time t_{d_d} of the equivalent triangular blast load is 18 ms
5 calculated using Equation (6). The peak pressure p_r is 261 kPa as calculated in step
6 (4) while the design impulse demand $\lambda \hat{i}_D$ is 2350 kPa·ms.
- 7 - Steps (10) and (11): the design is carried out using the equivalent single degree of
8 freedom. 0.93% of longitudinal reinforcing steel is needed in order to guarantee,
9 with 10% of *APE*, the moderate damage limit state under the design blast load
10 calculated in step (9). Figure 14(a) shows the RC panel resistance time history while
11 Figure 14(b) shows the RC panel deflection time history under the design blast load.
12 The considered equivalent single degree of freedom takes into account a flexural
13 failure only therefore the design for shear should be pertinently taken into account
14 in order to permit the development of the flexural mechanism. The shear demand
15 can be calculated from the flexural capacity (conservatively) or alternatively
16 directly from the single degree of freedom analysis.



1

2 Figure 14: Structural analysis results for the case study RC panel: (a) resistance and (b)
3 deflection (mid-span deflection) time history.

4

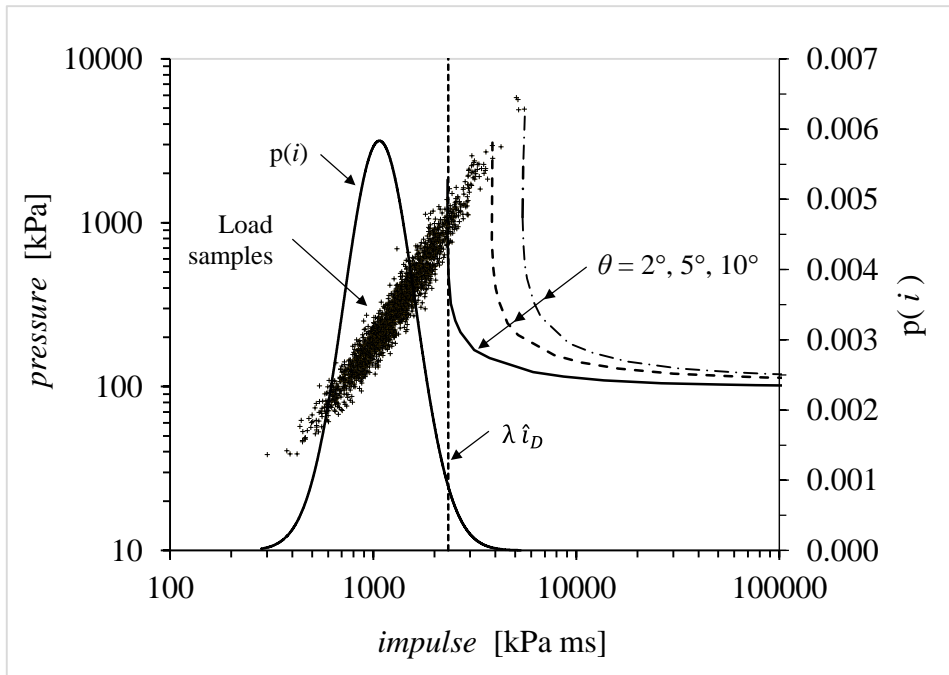
5 In order to validate the design carried out using the proposed safety factor λ , a Monte Carlo
6 simulation is used to accurately assess the probability of exceedance of the selected
7 moderate limit state. Different meanings can be given to a Monte Carlo simulation. In this
8 specific contest the Monte Carlo simulation calculates the probability of exceeding a limit
9 state by repeating a structural analysis and changing each time the parameters affected by
10 uncertainty in a range of values given by probability distributions. Then it counts the
11 number of structural analyses over the total where the response parameter exceeds the limit
12 state value. It is essentially a numerical procedure that utilizes samples of the random
13 variables, i.e., numerous possible scenarios, and solves each scenario to determine
14 acceptance or failure, and by statistics of the ensemble estimate the probability of failure.
15 For validating the design carried out using the proposed safety factor λ the structural model

1 used in the Monte Carlo simulation is the same equivalent SDOF adopted for designing the
2 RC panel with the safety factor λ and the uncertainties are in the load only. Also the mean
3 value of the stand-off distance \bar{R} and amount of explosive \bar{W} and their variability V_R and
4 V_W are the same. Furthermore in the sensitivity analysis the uncertainties affecting the
5 structural model (equivalent SDOF) are introduced as well. In particular the variability in
6 the concrete and steel strength are considered.

7 The Monte Carlo simulation gives a probability of exceedance of the moderate limit state
8 equal to 9.2% which is very close to the selected *APE* of 10%. The pressure–impulse
9 diagram of the designed RC panel has been plotted in Figure 15 together with the blast load
10 samples used in the Monte Carlo simulation. Generally the loading conditions (e.g.
11 impulsive, dynamic and quasi-static) of an element, as the considered RC panel, can change
12 in function of the response parameter value (limit state) because the resistance function is
13 nonlinear. The loading conditions of an element can be different in function of the
14 considered limit state (e.g dynamic region for elastic regime while impulsive region for a
15 plastic regime) because every limit state has a different pressure-impulse diagram.

16 Therefore a direct control of the loading condition on the pressure-impulse diagram is
17 always recommendable. Figure 15 shows that the hypothesis of impulsive loaded structure
18 is valid because the load samples are in the impulsive region of the pressure–impulse
19 diagram. Furthermore in the same figure the probability density function of the impulse
20 demand is also plotted together with the design impulse demand $\lambda \hat{i}_D$, which has been
21 essentially designed to become coincident with the median impulse capacity \hat{i}_C of the RC

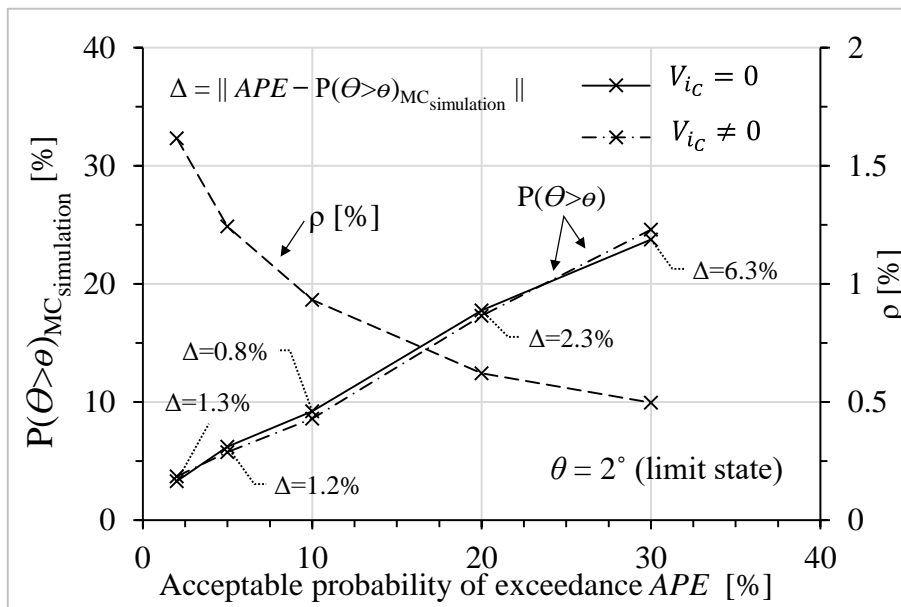
1 panel for a support rotation θ of 2 degrees. The pressure–impulse diagram shown in Figure
 2 15 are made using the SBEDS[®] software (US Army 2008).



3
 4 Figure 15: Pressure–impulse diagrams of the RC panel for the limit states corresponding to
 5 $\theta = 2^\circ, 5^\circ$ and 10° and the blast load samples are plotted over them; furthermore the PDF of
 6 the impulse is plotted as well together with the design impulse $\lambda \hat{i}_D$ (vertical dashed line).

7
 8 Finally a sensitivity analysis is presented in Figure 16. The probability of exceedance of the
 9 limit state, $P(\Theta > \theta)$, calculated using a Monte Carlo simulation is compared with the
 10 acceptable probability of exceedance APE selected in the design which is made using the
 11 safety factor λ . For the Monte Carlo simulation, capacity variability is also incorporated to
 12 verify the effect of neglecting it in the safety factor approach. Thus, the concrete and steel
 13 strength are considered lognormally distributed with a coefficient of variation of 0.18 and

1 0.12 respectively. As shown in Figure 16, this comparison validates the proposed safety
 2 factor λ because the probabilities of exceedance estimated with Monte Carlo simulations
 3 are close to the acceptable probabilities of exceedance APE selected in the design. The
 4 maximum difference Δ in computing the probability of exceedance is 6.3%, a value that
 5 only appears for large APE s in the order of 30%, which will probably not factor into a
 6 realistic design situation (Figure 16). In Figure 16 the minimum reinforcement percentage ρ
 7 of the panel is also plotted, as needed to satisfy the limit state for different values of APE .
 8 As expected, ρ follows the trend of the safety factor λ shown in Figure 5.



9

10 Figure 16: Probability of exceeding the limit state $P(\Theta > \theta)$ calculated using a Monte Carlo
 11 simulation compared with the APE used in the design carried out with the proposed safety
 12 factor λ . The structural uncertainties have been considered as well for comparison purpose.
 13 Furthermore the reinforcement percentage is plotted too as design output for the RC panel.
 14 The proposed approach is accurate enough for APE s < 15% while for higher APE s (not
 15 suitable for design purposes) it gives a conservative design.

1

2 **8 Conclusions**

3 A safety factor λ for structures subjected to impulsive blast loads has been presented as an
4 alternative to cumbersome probabilistic analyses carried out using Monte Carlo simulation.
5 In fact the design carried out using the proposed safety factor λ guarantees the acceptable
6 probability of exceedance *APE* of the structural performance (limit state) using current
7 practice design procedures because it only modifies the blast demand. The safety factor λ is
8 function of the acceptable probability of exceedance *APE*, and the lognormal distribution
9 parameters of the standoff distance and the explosive weight.

10 In summary the proposed safety factor λ , introduces the concept of acceptable reliability in
11 the design of components subjected to impulsive blast loads without increasing the
12 computational and human resources spent in design.

13 **9 Acknowledgements**

14 The content of this manuscript has been based on the work supported by the International
15 Research Fellow and KAKENHI (Grant-In-Aid) of the Japan Society for the Promotion of
16 Science under grant number P-15786. Any opinions, findings, and conclusions or
17 recommendations expressed in this article are those of the authors and do not necessarily
18 reflect the views of the Japan Society for the Promotion of Science. Furthermore the
19 support of Prof. Yukio Tamura (School of Civil Engineering, Beijing Jiaotong University,
20 China and Program Coordinator of WE-JURC at Tokyo Polytechnic University, Japan) and

1 Prof. Akihito Yoshida (Department of Architecture and Wind Engineering, Tokyo
2 Polytechnic University, Japan) is gratefully acknowledged. The Visiting Fellowship
3 provided to the first author by the Centre for Infrastructure Performance and Reliability at
4 The University of Newcastle (Australia) is also gratefully acknowledged.

5 **10 References**

- 6 AISC (2003). *LRFD Manual of Steel Construction, 3rd edition*, American Institute of
7 Steel Construction, Chicago, USA.
- 8 Biggs, J.M. (1964). *Introduction to structural dynamics*, McGraw-Hill, New York,
9 USA.
- 10 Chang, D.B., Young, C.S. (2010). “Probabilistic estimates of vulnerability to explosive
11 overpressures and impulses”, *Journal of Physical Security*, Vol. 4, No. 2, pp. 10-29.
- 12 Cornell, C.A. (1969). “A probability-based structural code”, *Journal of the American*
13 *Concrete Institute*, Vol. 66, No. 1.
- 14 Cornell, C.A., Jalayer, F., Hamburger, R.O., Foutch, D.A. (2002). “Probabilistic Basis
15 for 2000 SAC Federal Emergency Management Agency Steel Moment Frame
16 Guidelines”, *Journal of Structural Engineering*, Vol. 128, No. 4, pp. 526-533.
- 17 Gantes, C.J., Pnevmatikos, N.G. (2004). “Elastic–plastic response spectra for
18 exponential blast loading”, *International Journal of Impact Engineering*, Vol. 30, pp.
19 323-343.

- 1 Krauthammer, T. (2008). *Modern protective structures*. CRC Press, Taylor & Francis
2 Group, New York, USA.
- 3 Low, H.Y., Hao, H. (2001). “Reliability analysis of reinforced concrete slabs under
4 explosive loading”, *Structural Safety*, Vol. 23, pp. 157-178.
- 5 Luco, N., Cornell, C.A. (2000). “Structure-specific scalar intensity measures for near
6 source and ordinary earthquake ground motions”, *Earthquake Spectra*, Vol. 23, pp.
7 357–92.
- 8 Grant, M., Stewart, M.G. (2015). “Probabilistic risk assessment for improvised
9 explosive devices attacks that cause significant building damage”, *Journal of*
10 *Performance of Constructed Facilities*, Vol. 29, No. 5, B4014009.
- 11 Netherton, M.D., Stewart, M.G. (2009). “The effects of explosive blast load variability
12 on safety hazard and damage risks for monolithic window glazing”, *International*
13 *Journal of Impact Engineering*, Vol. 36, pp. 1346-1354.
- 14 Nickerson, J., Trasborg, P., Naito, C., Newberry, C., Davidson, J. (2015). “Finite
15 element evaluation of blast design response criteria for load-bearing precast wall
16 panels”, *International Journal of Protective Structures*, Vol. 6, No. 1, pp. 155-173.
- 17 Olmati, P., Petrini, F., Gkoumas, K. (2014). “Fragility analysis for the Performance-
18 Based Design of cladding wall panels subjected to blast load”, *Engineering Structures*,
19 Vol. 78, pp. 112–120.

- 1 Olmati, P., Petrini, F., Vamvatsikos, D., Gantes, C.J. (2016). “Simplified fragility-based
2 risk analysis for impulse governed blast loading scenarios”, *Engineering Structures*,
3 Vol. 117, pp. 457–469.
- 4 Parisi, F., Balestrieri, C., Asprone, D. (2016). “Blast resistance of tuff stone masonry
5 walls”, *Engineering Structures*, Vol. 113, pp. 233-244.
- 6 Shi, Y., Hao, H., Hao, Z.X. (2008). “Numerical derivation of pressure–impulse
7 diagrams for prediction of RC column damage to blast loads”, *International Journal of*
8 *Impact Engineering*. Vol. 35, pp. 1213-1227.
- 9 Shi, Y., Stewart, M.G. (2015a). “Spatial reliability analysis of explosive blast load
10 damage to reinforced concrete columns”, *Structural Safety*, Vol. 53, pp. 13-25.
- 11 Shi, Y. and Stewart, M.G. (2015b), Damage and Risk Assessment for Reinforced
12 Concrete Wall Panels Subject to Explosive Blast Loading, *International Journal of*
13 *Impact Engineering*, Vol. 85, pp. 5-19.
- 14 Stewart, M.G. (2008). “Cost-effectiveness of risk mitigation strategies for protection of
15 building against terrorist attack”, *Journal of Performance of Constructed Facilities*,
16 10.1061/(ASCE)0887-3828(2008)22:2(115), 115-120.
- 17 Stewart, M.G. (2010). “Risk-informed decision support for assessing the costs and
18 benefits of counter-terrorism protective measures for infrastructure”, *International*
19 *Journal of Critical Infrastructure Protection*, Vol. 3, No. 1, pp. 29-40.

- 1 Stewart, M.G. (2011). “Life-safety risks and optimisation of protective measures
2 against terrorist threats to infrastructure”, *Structure and Infrastructure Engineering*, Vol.
3 7, No. 6, pp. 431-440.
- 4 Stewart, M.G. (2012). “Integration of Uncertainty Modelling, Structural Reliability and
5 Decision Theory to Provide Optimal Blast Protection to Infrastructure”, *Advances in*
6 *protective structures research*, H. Hao and Z.X. Li, eds., CRC Press, London.
- 7 Stewart, M.G., Netherton, M.D., Shi, Y., Grant, M., Mueller, J. (2012). “Probabilistic
8 terrorism risk assessment and risk acceptability for infrastructure protection”,
9 *Australian Journal of Structural Engineering*, Vol. 13, No. 1, pp. 1-18.
- 10 Stewart, M.G, Mueller, J. (2014). “Terrorism risk for bridges in a multi-hazard
11 environment”, *International Journal of Protective Structures*, Vol. 5, No. 3, pp. 275-289.
- 12 Stewart, M.G., Netherton, M.D. (2015). “Reliability-based design load factors for
13 explosive blast loading”, *Journal of Performance of Constructed Facilities*, Vol. 29, No.
14 5, B4014010.
- 15 Stochino, F., Carta, G. (2014). “SDOF models for reinforced concrete beams under
16 impulsive loads accounting for strain rate effects”, *Nuclear Engineering and Design*,
17 Vol. 276, pp. 74-86.
- 18 The Federal Emergency Management Agency - FEMA (2005). *Risk assessment a how*
19 *to guide to mitigate potential terrorist attacks against buildings, providing protection to*
20 *people and buildings*.

- 1 U.S. Army (2008). *Methodology Manual for the Single-Degree-of-Freedom Blast*
2 *Effects Design Spreadsheets*, United States Army Corps of Engineers, Washington, DC.
- 3 DoD (Department of Defense) (2008). *Structures to resist the effects of accidental*
4 *explosions*, Unified Facilities Criteria (UFC) 3-340-02, Washington, DC.
- 5 Yokohama, H., Sunde, J., Ellis-Steinborner, S.T., Ayubi, Z. (2015). “Vehicle Borne
6 Improvised Explosive Device (VBIED). Characterization and Estimation of its Effects
7 in Terms of Human Injury”, *International Journal of Protective Structures*, Vol. 6, No.
8 4, pp. 607-627.
- 9